Spectrum Width Estimators for the NEXRAD ORDA: Evaluation and Recommendation

GREGORY MEYMARIS*

National Center for Atmospheric Research, Boulder, Colorado

JOHN K. WILLIAMS

National Center for Atmospheric Research, Boulder, Colorado

1. INTRODUCTION

With the advent of the Open Radar Data Acquisition (ORDA) system on WSR-88D radars and the introduction of significantly more powerful signal processing hardware comes the opportunity to improve the method used for estimating the spectrum width, a measure of the variability of radial wind velocities within a measurement pulse volume. In addition, the implementation of new operational modes for improved data quality, including SZ phase coding, will involve very different signal processing techniques and hence may require novel methods to meet the WSR-88D specifications. While spectrum width has not been used extensively by radar meteorologists in the past, the new NEXRAD Turbulence Detection Algorithm (NTDA), developed under direction and funding from the FAA's Aviation Weather Research Program, will soon be using the WSR-88D spectrum width as a key input for providing in-cloud turbulence estimates (eddy dissipation rate, EDR) for an operational aviation decision support system (Williams et al. 2005). Achieving improved spectrum width estimator performance would directly benefit the accuracy of the NTDA product.

This paper addresses these issues by evaluating performance characteristics of several spectrum width estimators, including the pulse-pair estimator currently used in the WSR-88D. Evaluations are performed using simulated radar timeseries data representing a variety of scenarios for different signal-to-noise ratios, overlaid power ratios, and spectrum widths. A hybrid algorithm combining three spectrum width estimators is proposed, and it is shown that this algorithm, while somewhat more computationally intensive, is more accurate and robust than any method alone.

Corresponding author address:
Gregory Meymaris, RAL, NCAR
1850 Table Mesa Dr., Boulder, CO 80305
E-mail: meymaris at ucar.edu

2. Methodology

To evaluate and compare different spectrum width estimators we generated random complex timeseries data for various true spectrum width, signal-to-noise ratio (SNR) and overlaid power ratio (PR) scenarios. We used an I&Q simulation technique based on the method described in Frehlich and Yadlowsky (1994); Frehlich (2000); Frehlich et al. (2001) except that the autocorrelation function is that of a weather echo as defined as in Doviak and Zrnić (1993, p. 125). This is a preferable method for generating complex timeseries with a given average autocorrelation function, as opposed to what is described by Zrnić (1975), because it is not necessary to generate as long of a timeseries in order to get the correct temporal statistics.

In this study, we used the simulator to generate both long pulse repetition time (PRT) and short PRT data. We created one set of 5000 long PRT timeseries, with a PRT of 3106 μs ($Nyquist\ velocity\ V_a \approx 8\ m/sec$) for 16 samples, as well as two sets of 5000 short PRT timeseries, with a PRT of 913 μs ($V_a \approx 27\ m/sec$) for 43 samples. The long PRT data and the first set of the short PRT data were modulated by varying amounts and to each was added Gaussian white noise so as to generate data with specific SNRs. The second set of short PRT data was also modulated to varying amounts relative to the first set so as to generate a weaker overlaid trip with specific PRs, that is, ratios of the strong trip to the weak trip power. These simulated data correspond to the long and short PRT scans of the lowest two elevations ($0.5°$ and $1.5°$) of NEXRAD volume control pattern (VCP) 12, which is often used for observing convective weather, with the pulse repetition frequency (PRF, equals 1/PRT) #6. These settings represent a difficult case scenario for spectrum width estimators in particular because the radar dwell time is quite short in VCP 12. The WSR-88D's wavelength of 10 cm was assumed. In the scenarios in which the short PRT data has overlaid echoes, the spectrum widths of the strong trip (the

long PRT data and the first set of the short PRT data) were varied from 0.5 to 16 m/sec and the SNRs from 0 to 70 dB. For the weak trip (the second set of short PRT data), the velocities were randomized, the spectrum width was set to 4 m/sec, and the PRs were varied from 10 to 30 dB below the strong trip.

In what follows, the simulator input ("true") spectrum width will be denoted as W, while the estimated spectrum width will be denoted as $\hat{W}$ with a modifying subscript specifying the estimation technique used. Estimation errors were calculated by subtracting the simulator input values from the estimated values (i.e. $\hat{W} - W$). In this paper, we do not create plots of standard errors (i.e., RMS errors); rather, we break out the error analysis into biases and standard deviations, which have quite different implications for turbulence detection since bias cannot be mitigated by averaging while random deviations can. However, RMS error estimates may be obtained by taking the square root of the sum of the squared biases and standard deviations.

3. Standard Spectrum Width Estimators

For simplicity, in this paper we only consider three standard spectrum width estimators. During our simulation studies, we evaluated several others, but these three are widely known, are computationally tractable, and they performed well under certain circumstances, allowing the formation of an effective hybrid method.

a. *The short PRT $R0/R1$ Pulse Pair Estimator*

The standard spectrum width estimator currently used in the WSR-88D radars on short PRT data is the $R0/R1$ estimator (Doviak and Zrnić 1993), so named because it utilizes the ratio of the first two lags of the autocorrelation function:

$$\hat{W}_{s01} = \left(\sqrt{2}/\pi\right) V_a \left|\log\left(P_S/|R_1|\right)\right|^{1/2} \qquad (1)$$

The "s" in the subscript "s01" indicates that the short PRT data are used. Here V_a is the Nyquist velocity, P_S is the average power of the signal with noise removed, and R_1 is the first lag of the autocorrelation function (i.e. $R_1 = (n-1)^{-1} \sum_{k=1}^{n-1} V^*(k) V(k+1)$ where $V(k)$ are the complex-valued I&Q radar timeseries). In the event that $|R_1| < P_S$, in which case the log has a negative argument, the spectrum width is set to 0 as is done on the WSR-88D.

The performance statistics obtained via simulation for the short PRT (913 μs) $R0/R1$ spectrum width estimator in the case of (essentially) no overlaid echoes is shown in Figure 1 for various input spectrum widths and SNRs. The biases are shown in Figure1(a), and the standard deviation of the errors $\hat{W}_{s01} - W$ is depicted in 1(b). The error standard deviation plot agrees reasonably well with that in Doviak and Zrnić (1993), although there are some differences. These may be caused by different approaches to

dealing with the cases where $|R_1| < P_S$, or to different methods used to generate timeseries segments for analysis. The biases and standard deviations show that for low SNRs (0 and 4 dB) this estimator is very poor, with large error standard deviations and large and variable bias values. As SNR increases to 10 dB and greater, the bias relative to the input spectrum width improves dramatically for all but rather small or quite large input spectrum widths, and the error standard deviations improve for small and, especially, medium spectrum width values. For large input spectrum widths, the spectrum width estimator eventually saturates, as can be seen from the increasing negative bias for all SNR levels.

b. *The short PRT $R1/R2$ Pulse Pair Estimator*

Another estimator described by Doviak and Zrnić (1993) is the $R1/R2$ estimator, which is based on the ratio of the first and second lags of the autocorrelation function:

$$\hat{W}_{s12} = \left(2/\left(\pi\sqrt{6}\right)\right) V_a \left|\log\left(|R_1/R_2|\right)\right|^{1/2} \qquad (2)$$

where R_2 is the second lag of the autocorrelation function (i.e. $R_2 = (n-2)^{-1} \sum_{k=1}^{n-2} V^*(k) V(k+2)$. In the event that $|R_2| < |R_1|$, the spectrum width is set to 0.

The performance statistics obtained via simulation for the short PRT (913 μs) $R1/R2$ spectrum width estimator in the case of (essentially) no overlay for various input spectrum widths and SNRs is shown in Figure 2. The biases are shown in Figure2(a), and the error standard deviation in 2(b). The biases and error standard deviations show that for 0 dB SNR this estimator is very poor, but the performance for 4 dB is much improved over the $R0/R1$ estimator. Again, there are biases for small input spectrum widths, but the performance is significantly better than the $R0/R1$ estimator in this regime, particularly for SNRs of 10 dB or higher. In fact, the estimator as a whole performs better than $R0/R1$ until the input spectrum width approaches 8 m/sec. At that point the $R1/R2$ estimator saturates, leading to severe negative biases.

c. *The long PRT $R1/R2$ Pulse Pair Estimator*

For the lowest elevations tilts on the WSR-88D, a long PRT scan is followed by a short PRT scan in a "split cut" strategy that produces reflectivity estimates from the long PRT data and velocity and spectrum width estimates from the short PRT data. Currently, the long PRT data is not used in the Doppler moment estimates, but it is in principle available for this purpose. Thus, while not strictly a *different* estimator than the short PRT $R1/R2$ estimator described in section b, the long PRT $R1/R2$ estimator provides a separate estimate of the spectrum width having different performance characteristics due to the different PRT. The equation is the same as 2, except that we will denote this estimator as $\hat{W}_{L12}$ ("L" for long PRT).

The performance statistics obtained via simulation of the long PRT (3106 μs) $R1/R2$ spectrum width estimator in the case of (essentially) no overlay for various input
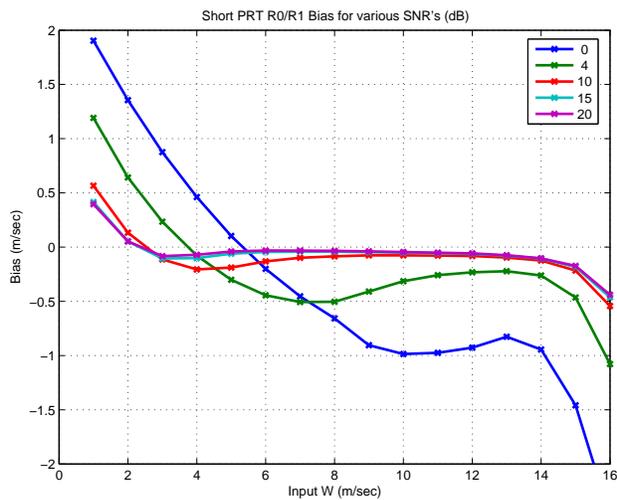
(a) Bias of $\hat{W}_{s01}$
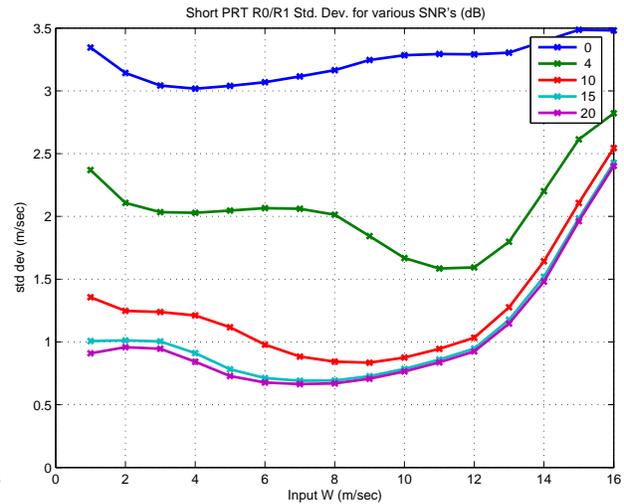
(b) Standard Deviation of $\hat{W}_{s01}$

Figure 1: Bias and error standard deviation plots of the short PRT $R0/R1$ spectrum width estimator for varying input spectrum widths and SNRs (0, 4, 10, 15 and 20 dB shown). The PR in this data is set at 30 dB, low enough such that the weak trip does not significantly impact the statistics.
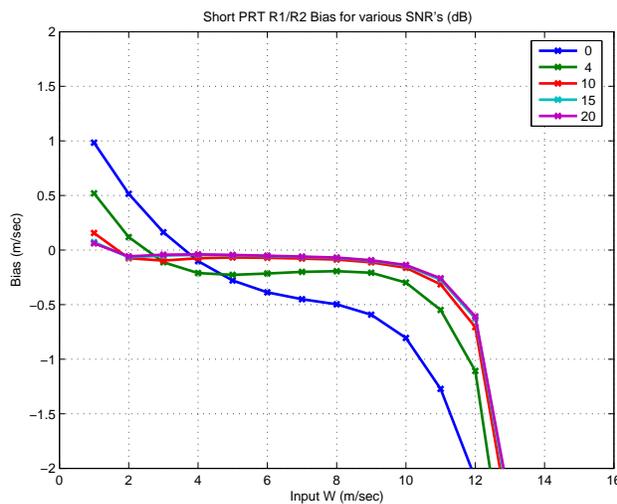
(a) Bias of $\hat{W}_{s12}$
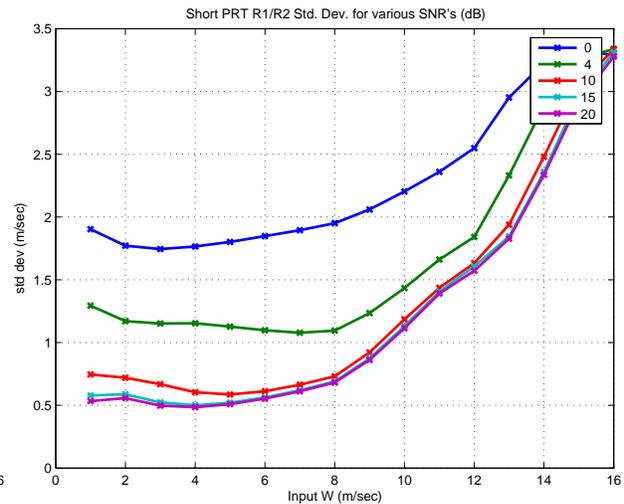
(b) Standard Deviation of $\hat{W}_{s12}$

Figure 2: Bias and error standard deviation plots of the short PRT $R1/R2$ spectrum width estimator for varying input spectrum widths and SNRs (0, 4, 10, 15 and 20 dB shown). The PR in this data is set at 30 dB, low enough that the weak trip does not significantly impact the statistics.

spectrum widths and SNRs is shown in Figure 3. The biases are shown in Figure3(a), and the error standard deviations in 3(b). The biases and error standard deviations show that for SNRs of 0 and 4 dB this estimator is very poor overall. However, as opposed to $\hat{W}_{s01}$ and $\hat{W}_{s12}$, this estimator has no bias for small spectrum widths down to 0.5 m/sec. Also, the error standard deviations are quite good, performing better than the $R0/R1$ estimator in this regime. In fact, on the whole the long PRT $R1/R2$ estimator performs better than the short PRT $R0/R1$ estimator until the input spectrum width approaches 3 m/sec, at which point the long PRT $R1/R2$ estimator saturates.

4. A Hybrid Approach

Taking the results from the three estimators ($\hat{W}_{s01}$, $\hat{W}_{s12}$, and $\hat{W}_{L12}$) together, it is seen that each performs well in certain regimes. $\hat{W}_{s01}$ performs well in higher SNRs and for larger spectrum widths, whereas $\hat{W}_{s12}$ performs well for slightly lower SNRs and medium-valued spectrum widths. The estimator $\hat{W}_{L12}$ performs the best for very narrow spectrum widths. These complementary regimes of relatively good performance suggest that a hybrid approach where all estimators are appropriately combined, might achieve good overall performance. There are many different ways that this combination could be done, but we have chosen to use a simple fuzzy logic-type approach. To wit, we define

$$\hat{W}_H = C_{s01}\hat{W}_{s01} + C_{s12}\hat{W}_{s12} + C_{L12}\hat{W}_{L12} \quad (3)$$

where the weights C_{s01}, C_{s12}, and C_{L12} may depend on various parameters, for instance, the input spectrum width, W, as well as SNR and PR. This is not a practical algorithm, of course, since we are using the input spectrum width, W, which wouldn't be available in practice and in fact is exactly what we are attempting to estimate. We get around this by using an initial estimate of W to retrieve the ideal weights, which are then used to in 3 to calculate the final estimate.

a. *Generating the Combination Weights*

As mentioned in section 2, we simulated short PRT timeseries data for various SNRs, PRs and input spectrum widths. Accompanying each simulation of the short PRT timeseries is a long PRT series with the same SNR and input spectrum width, but with no overlaid echoes. For each regime (i.e., values of spectrum width, SNR and PR) we generated 5000 overlaid short PRT time series and 5000 non-overlaid long PRT timeseries . Using these data, the mean and error standard deviation of each estimator can be calculated for each regime.

It can be shown that if n uncorrelated random variables X_i, $i = 1, \ldots, n$, have variances σ_i^2, then the weights C_i satisfying $0 \leq C_i \leq 1$ and $\sum_{i=1}^n C_i = 1$ that minimize the

variance of $\sum_{i=1}^n C_i X_i$ are defined by

$$= \frac{\prod_{k \neq i} \sigma_k^2}{\sum_{j=1}^n \prod_{k \neq j} \sigma_k^2} \quad (4)$$

The product $\prod_{k \neq i}$ is short hand for $\prod_{k=1, k \neq i}^n$. While this suggests a principled approach to generating the weights, it has a serious deficiency in that it does not address the fact that we want to minimize bias as well. Therefore, the following ad-hoc metric was used instead:

$$\epsilon = 10B^2 + S^2 \quad (5)$$

where B is the average bias and S is the error standard deviation (not standard error) for the estimator. For each SNR, PR and spectrum width regime and spectrum width estimator, ϵ is calculated. The weights for that regime are then calculated using 4, where ϵ is substituted for the σ_k^2 values (i.e. ϵ_{s01} is substituted for σ_1^2, etc.).

While the choice of 5 is somewhat arbitrary, it does have the desired attributes of strongly penalizing spectrum width estimators for biases while also penalizing for large variances. The factor 10 was chosen simply by trial and error. There are certainly more rigorous choices for computing optimal weights, and these will be explored in future work.

b. *Hybrid Algorithm using Optimal Weights*

Using the weights generated in section a, a new hybrid spectrum width estimator $\hat{W}_H$ is computed by the following algorithm:

1. Compute the 3 estimators $\hat{W}_{s01}$, $\hat{W}_{s12}$, and $\hat{W}_{L12}$

2. Look up the weights for the 3 estimators based on W, SNR, and PR

3. Calculate the hybrid spectrum width estimator using 3.

As mentioned before, this estimator can only be computed when performing simulation studies since that is the only time that the input spectrum width W is *known*. In the next section, we propose a hybrid algorithm in which we do not assume that W is known. The $\hat{W}_H$ estimator because it serves as a 'best case' scenario for the performance of the hybrid approach when the appropriate weights must be guessed.

c. *Hybrid Algorithm using an Initial Seed*

The obvious approach to dealing with the fact that W is unknown is to simply use one of the estimators $\hat{W}_{s01}$, $\hat{W}_{s12}$, or $\hat{W}_{L12}$ as a proxy for W in finding the combination weights. After all, these estimates will need to be computed anyway. On the other hand, no one of these algorithms performs very well in all situations. Experiments using either $\hat{W}_{s12}$ or $\hat{W}_{s12}$ as a proxy for W resulted in very poor performance. The use of $\hat{W}_{L12}$ as a proxy for W is not feasible since it saturates for fairly small spectrum

(a) Bias of $\hat{W}_{L12}$ (b) Standard Deviation of $\hat{W}_{L12}$
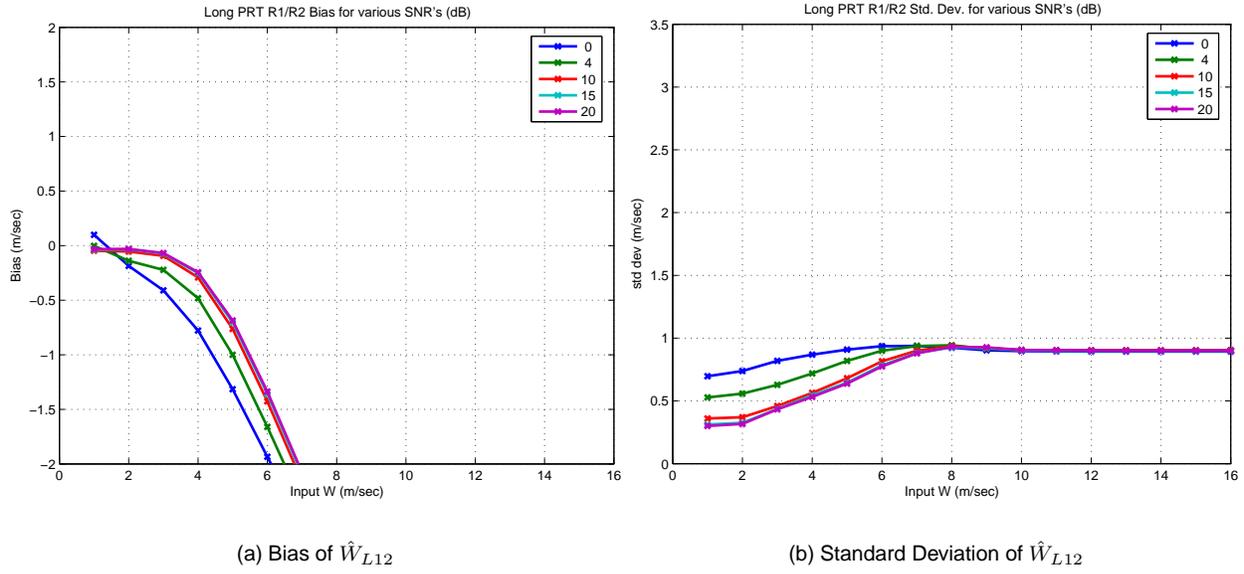
Figure 3: Bias and error standard deviation plots of the long PRT $R1/R2$ spectrum width estimator for varying input spectrum widths and SNRs (0, 4, 10, 15 and 20 dB shown). The PR in this data is set at 30 dB, low enough such that the weak trip does not impact the statistics.

widths. The approach that we settled on was a heuristic estimator defined by the following:

$$\hat{W}_S = \begin{cases} \hat{W}_{s01} & \text{if } \hat{W}_{s01} > T_1 \\ \hat{W}_{s12} & \text{if } \hat{W}_{s01} \le T_1 \text{ and } \hat{W}_{s12} > T_2 \\ \hat{W}_{L01} & \text{if } \hat{W}_{s01} \le T_1, \hat{W}_{s12} \le T_2 \end{cases} \quad (6)$$

where for this study we chose $T_1 = 7\,m/sec$ and $T_2 = 2\,m/sec$.

Thus we define a new estimator, $\hat{W}_{\hat{H}}$, which is computed using the following algorithm:

1. Compute the 3 estimators $\hat{W}_{s01}$, $\hat{W}_{s12}$, and $\hat{W}_{L12}$
2. Compute $\hat{W}_S$ using 6
3. Look up the weights for the 3 estimators based on $W = \hat{W}_S$, SNR, and PR
4. Calculate $\hat{W}_{\hat{H}}$ as in 3.

Unlike $\hat{W}_H$, the estimator $\hat{W}_{\hat{H}}$ uses only information available from measured parameters and is therefore a practical algorithm for an operational radar.

5. Results

Performance comparison plots for the five spectrum width estimators ($\hat{W}_{s01}$, $\hat{W}_{s12}$, $\hat{W}_{L01}$, $\hat{W}_H$, and $\hat{W}_{\hat{H}}$) are shown in Figures 4-10. Biases as a function of spectrum width are shown in the top panel of each figure, and the error standard deviations in the middle. The weights applied to each of the standard spectrum widths ($\hat{W}_{s01}$, $\hat{W}_{s12}$, and $\hat{W}_{L01}$) for a given input spectrum width (W in the case of $\hat{W}_H$, and estimated by $\hat{W}_S$ in the case of $\hat{W}_{\hat{H}}$), are shown in the bottom plot.

a. *Non-overlaid case*

Results for the simulated cases containing essentially no overlaid echoes (that is, 30 dB PR) for SNRs of 4, 10, and 70 dB, respectively, are shown in Figures 4, 5, and 6. In general, the seeded hybrid estimator $\hat{W}_{\hat{H}}$ outperforms the other estimators with the exception of the idealized $\hat{W}_H$. For 4 dB SNR and low input spectrum widths, some improvement is still desired as the seeded hybrid estimator becomes biased high and has error standard deviations that are worse than both $\hat{W}_{s12}$ and $\hat{W}_{L01}$, although it still performs better than $\hat{W}_{s01}$.

For 10 dB SNR, the performance almost perfectly tracks the best parts of each of the three original spectrum width estimators ($\hat{W}_{s01}$, $\hat{W}_{s12}$, and $\hat{W}_{L01}$), except for the case with spectrum width of 0.5 m/sec. $\hat{W}_{L12}$ still performs best for very narrow spectrum widths. For the 70 dB SNR case, the seeded hybrid algorithm performs essentially as the best parts of each algorithm, outperforming $\hat{W}_{s01}$ for narrow spectrum widths.

b. *Overlaid case with a power ratio of 10 dB*

Results for the simulated cases containing overlaid echoes at 10 dB PR are shown in Figures 7 and 8 for SNRs of 4 dB and 10 dB, respectively. All of the estimators perform very poorly in general for the 4 dB SNR case. The seeded algorithm does not perform very well in this case, but it is the most consistent of the group. The $\hat{W}_{s12}$ estimator has

good performance when the spectrum width is less than 6 m/sec, at which point it starts to saturate. The $\hat{W}_{s01}$ estimator is almost always badly biased.

In the 10 dB SNR case, $\hat{W}_{\hat{H}}$ exhibits a minor bias throughout except when the input spectrum widths are small, where it becomes significant. $\hat{W}_{s01}$, however, has a consistently worse bias. $\hat{W}_{L01}$ performs better for very small spectrum widths. Larger SNRs are not shown here but the performance of all the estimators are largely unchanged from the 10dB SNR case.

c. *Overlaid case with a power ratio of 14 dB*

The 14 dB PR results are shown in Figures 9 and 10 for SNRs of 4 dB and 10 dB, respectively. Again, larger SNRs are not shown since the spectrum width estimator performances are similar to those at 10 dB SNR. The seeded hybrid estimator performs well, though there is still room for improvement in the 4 dB SNR case. Again, it outperforms $\hat{W}_{s01}$ for smaller spectrum widths, but the $\hat{W}_{s12}$ estimator outperforms both of them in this regime.

In the 10 dB SNR case, the seeded hybrid spectrum width estimator performs very well, although some improvement may be possible for narrow spectrum widths, where there is a bias, and especially at 0.5 m/sec, where there is a spike in the error standard deviation. Again, $\hat{W}_{L01}$ performs better for very small spectrum widths.

6. Conclusions

The simulation results presented in this paper have shown that the short PRT $R0/R1$ spectrum width estimator currently used on WSR-88Ds does not perform as well as the short or long PRT $R1/R2$ estimators in certain regimes. A hybrid approach that combines these methods using weights appropriate to each regime shows great promise in producing improved overall performance. While knowledge of the true spectrum width would allow determining the ideal combination weights, an alternative that uses a spectrum width estimate, or "seed", based on the values of the three spectrum width estimators was proposed as a practical alternative. The seeded hybrid estimator presented in this paper was shown to outperform all three spectrum width estimators in most cases, and at the least did no worse than the short PRT $R0/R1$ estimator currently used by the WSR-88D. For larger spectrum widths, it outperforms the short and long PRT $R1/R2$ estimators, but for low spectrum widths and low SNRs and/or PRs they in turn outperform the seeded hybrid estimator. Fortunately, this is the domain least importance for a turbulence warning capability. Computationally, the seeded hybrid algorithm is fairly modest, requiring fewer operations than the FFT needed by a spectral technique. The biggest requirement would be the memory needed to store the table of combination weights for the weighted sum, since weights would be required for each of the different spectrum width, SNR, and PR regimes.

Future work includes improving the performance for small spectrum widths, where the less than optimal quality seems to be due to the poor estimation of the seed spectrum width $\hat{W}_S$. That this is the source of the poor performance can be seen by the fact that if the simulation *input* spectrum width is used, as in $\hat{W}_H$, the resulting estimator's performance is superior to any one algorithm. Thus, the algorithm for the seed spectrum width will be further refined. In addition, other spectrum width estimators such as spectral or maximum likelihood methods could easily be integrated into the general framework developed here, and this hybrid approach can be applied to other VCPs including those that involve phase-coded signals. It is our recommendation that the hybrid estimator approach be further refined and then considered for implementation in the WSR-88D Open Radar Data Acquisition system.

7. Acknowledgements

References

Doviak, R. J. and D. S. Zrnić: 1993, *Doppler Radar and Weather Observations*, Academic Press, San Diego, California. 2nd edition.

Frehlich, R., 2000: Simulation of coherent doppler lidar performance for space-based platforms. *Journal of Applied Meteorology*, **39**, 245–262.

Frehlich, R., L. B. Cornman, and R. Sharman, 2001: Simulation of three-dimensional turbulent velocity fields. *Journal of Applied Meteorology*, **40**, 246–258.

Frehlich, R. and M. J. Yadlowsky, 1994: Performance of mean-frequency estimators for doppler radar and lidar. *Journal of Atmospheric and Oceanic Technology*, **11**, 1217–1230, corrigenda, **12**, 445–446.

Williams, J. K., L. Cornman, J. Yee, S. G. Carson, and A. Cotter: 2005, Real-time remote detection of convectively-induced turbulence. AMS 32nd Radar Meteorology Conference, Albuquerque, NM.

Zrnić, D. S., 1975: Simulation of weatherlike doppler spectra and signals. *Journal of Applied Meteorology*, **14**, 619–620.
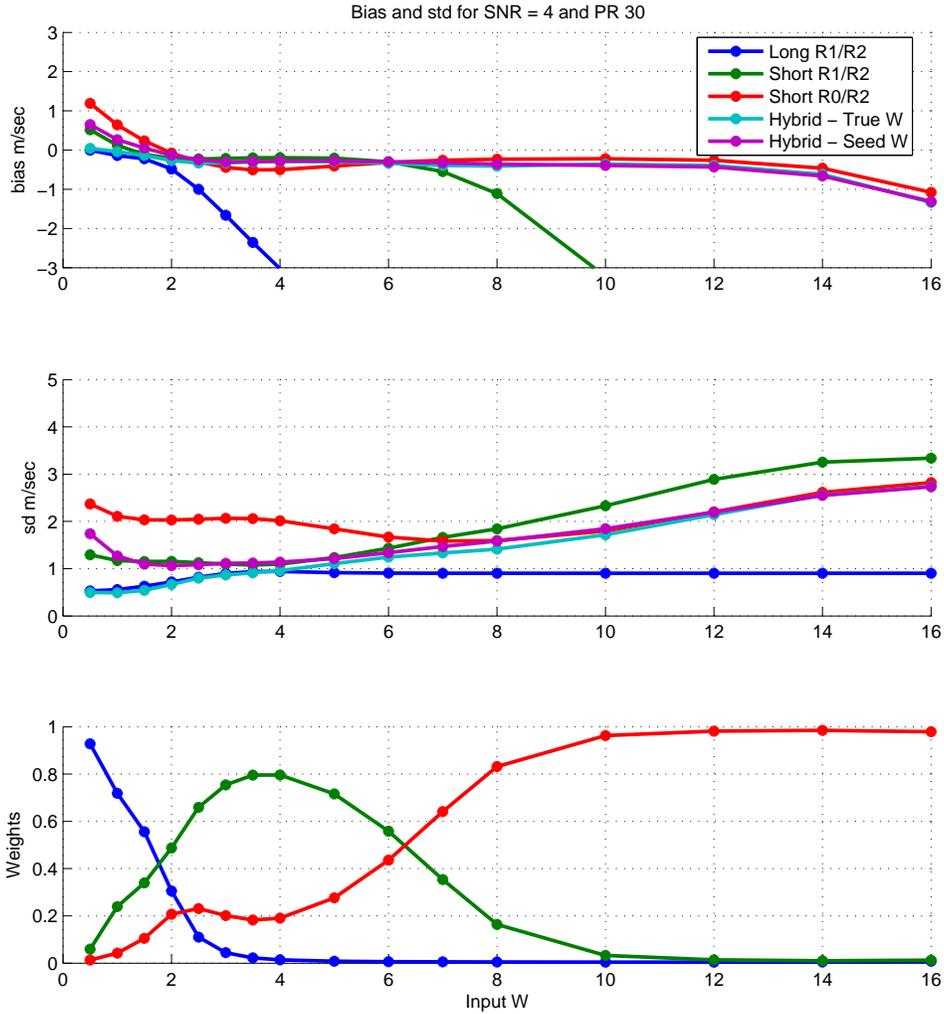
Figure 4: Performance statistics plots for 4 dB SNR and 30 dB PR, for the short PRT $R1/R2$ ($\hat{W}_{s12}$)and $R0/R1$ ($\hat{W}_{s01}$), long PRT $R1/R2$ ($\hat{W}_{L12}$), and the hybrid estimators $\hat{W}_H$ and $\hat{W}_{\hat{H}}$. Biases as a function of input spectrum width are shown in the top panel, the error standard deviations in the middle, and the weights used for the hybrid estimators in the bottom. Note that the "input" W for the $\hat{W}_{\hat{H}}$estimator is $\hat{W}_S$, whereas for $\hat{W}_H$ the simulator input W is used.
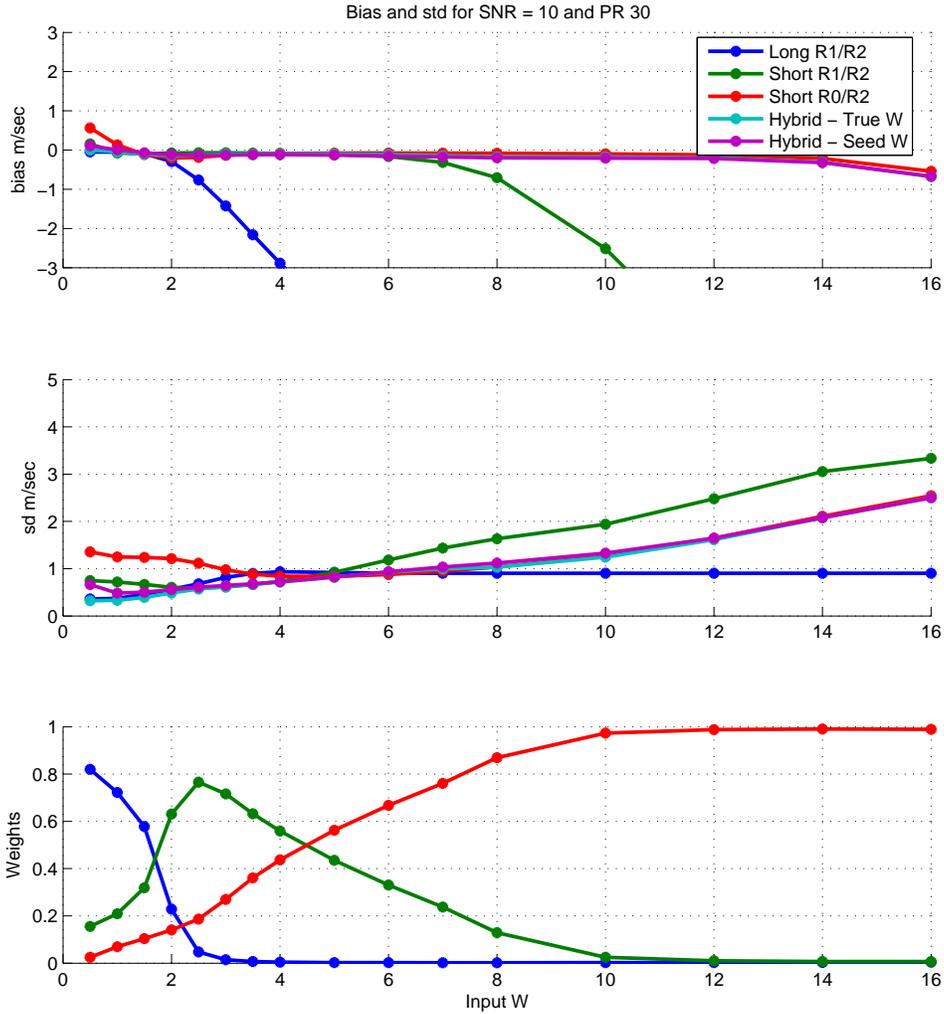
Figure 5: Performance statistics for 10 dB SNR and 30 dB PR, for the short PRT $R1/R2$ ($\hat{W}_{s12}$) and $R0/R1$ ($\hat{W}_{s01}$), long PRT $R1/R2$ ($\hat{W}_{L12}$), and the hybrid estimators $\hat{W}_H$ and $\hat{W}_{\hat{H}}$. Biases as a function of input spectrum width are shown in the top panel, the error standard deviations in the middle, and the weights used for the hybrid estimators in the bottom. Note that the "input" W for the $\hat{W}_{\hat{H}}$ estimator is $\hat{W}_S$, whereas for $\hat{W}_H$ the simulator input W is used.
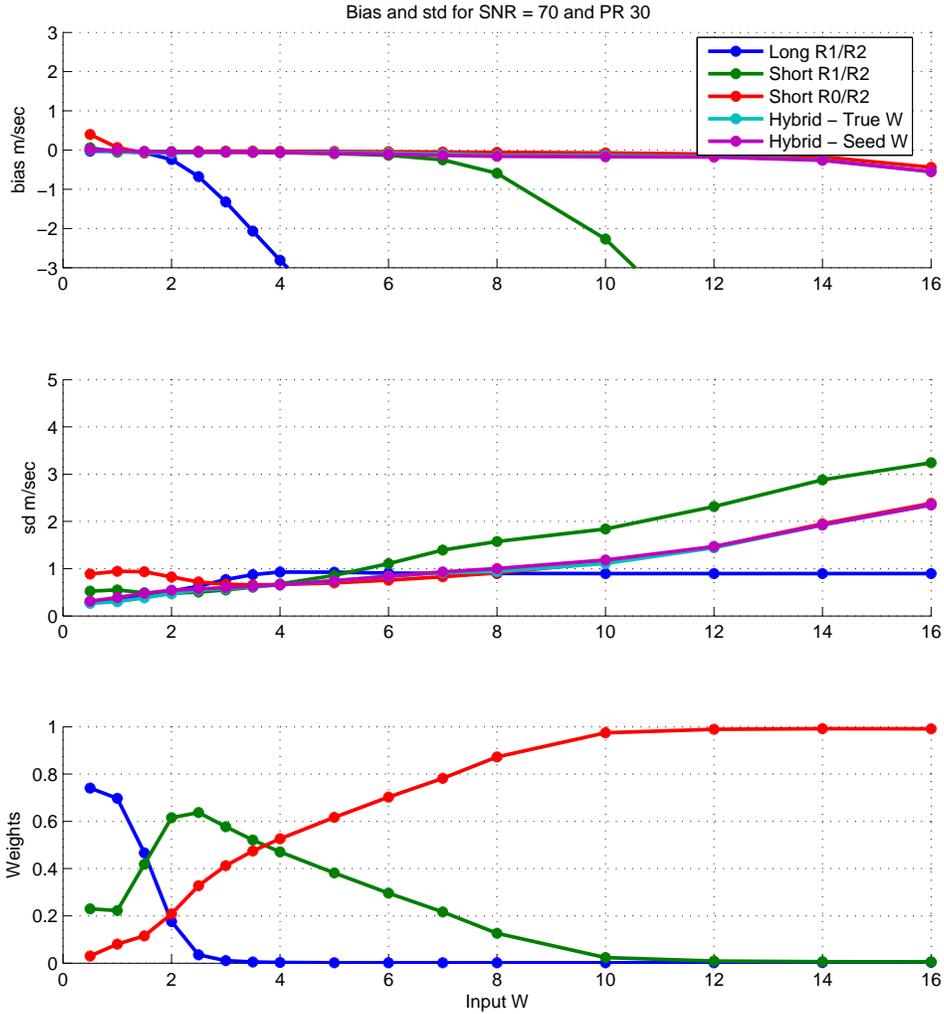
Figure 6: Performance statistics for 70 dB SNR and 30 dB PR, for the short PRT $R1/R2$ ($\hat{W}_{s12}$)and $R0/R1$ ($\hat{W}_{s01}$), long PRT $R1/R2$ ($\hat{W}_{L12}$), and the hybrid estimators $\hat{W}_H$ and $\hat{W}_{\hat{H}}$. Biases as a function of input spectrum width are shown in the top panel, the error standard deviations in the middle, and the weights used for the hybrid estimators in the bottom. Note that the "input" W for the $\hat{W}_{\hat{H}}$ estimator is $\hat{W}_S$, whereas for $\hat{W}_H$ the simulator input W is used.
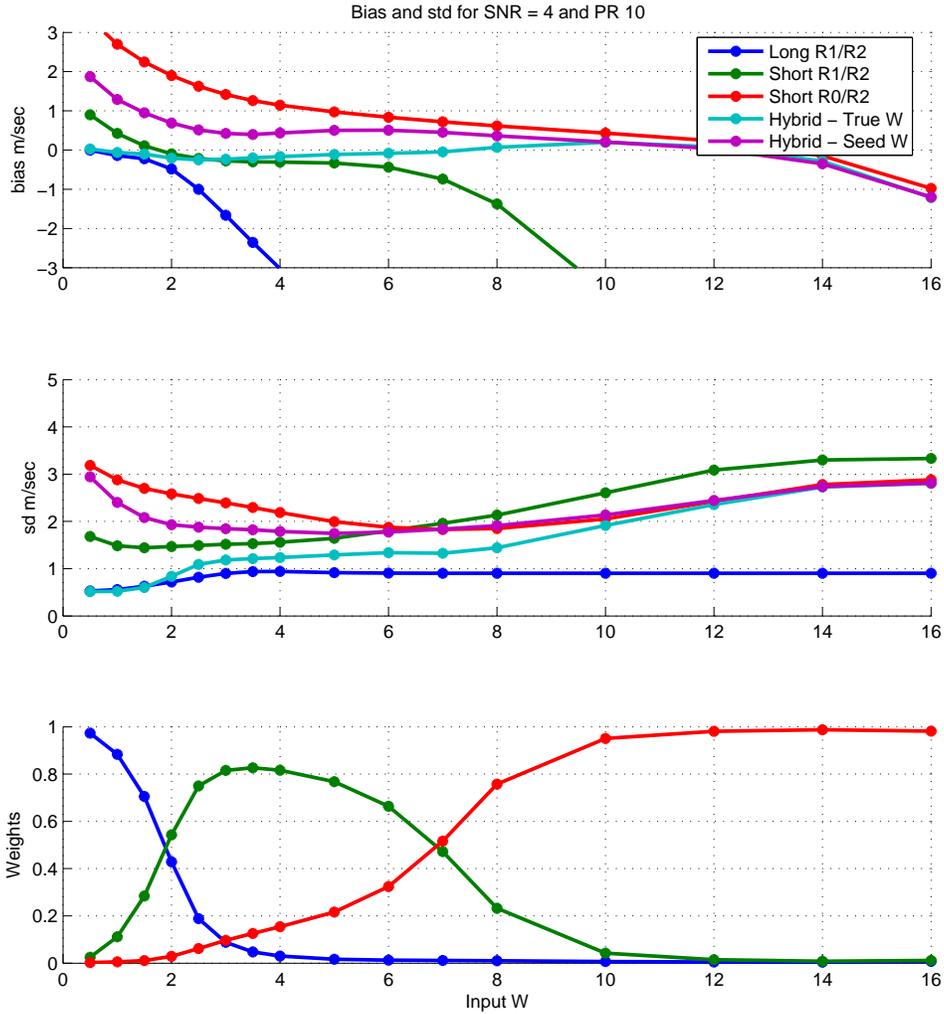
Figure 7: Performance statistics plots for 4 dB SNR and 10 dB PR, for the short PRT $R1/R2$ ($\hat{W}_{s12}$) and $R0/R1$ ($\hat{W}_{s01}$), long PRT $R1/R2$ ($\hat{W}_{L12}$), and the hybrid estimators $\hat{W}_H$ and $\hat{W}_{\hat{H}}$. Biases as a function of input ("true") spectrum width are shown in the top panel, the error standard deviations in the middle, and the weights used for the hybrid estimators in the bottom. Note that the "input" W for the $\hat{W}_{\hat{H}}$ estimator is the "seed" $\hat{W}_S$ described in the text, whereas for $\hat{W}_H$ the simulator input W is used.
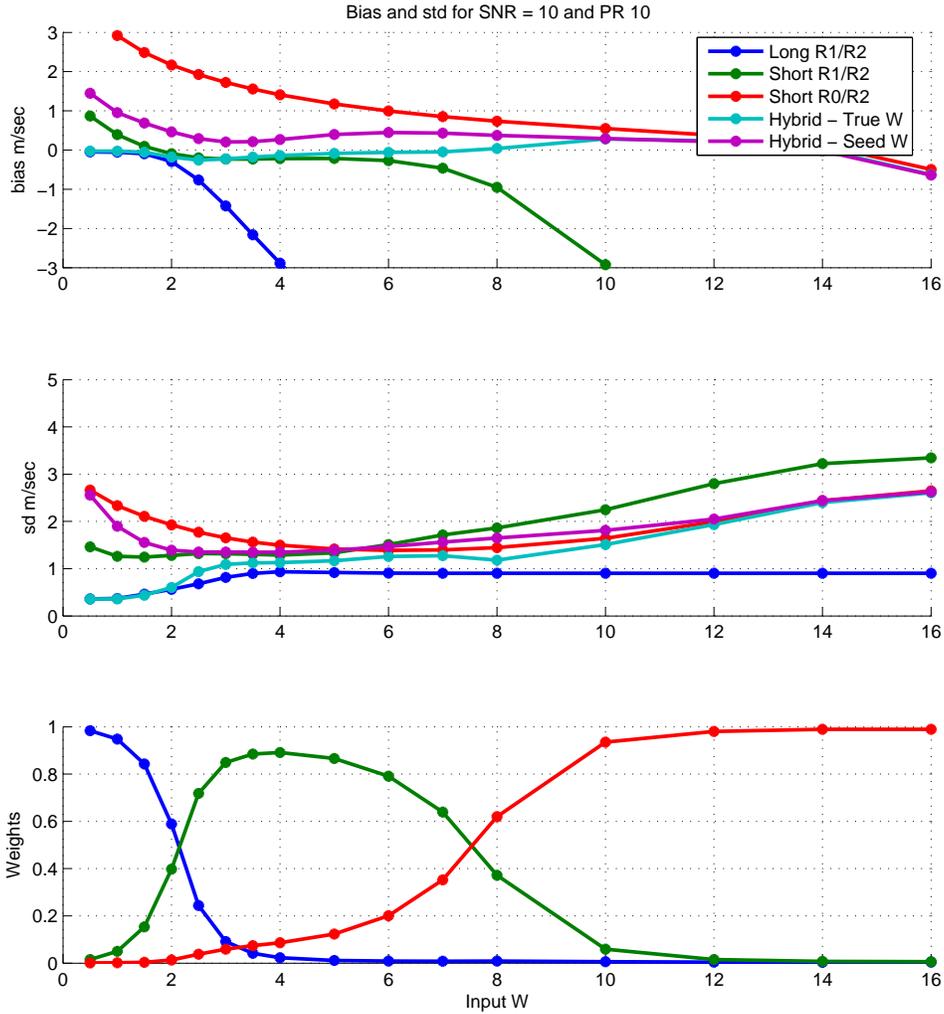
Figure 8: Performance statistics plots for 10 dB SNR and 10 dB PR, for the short PRT $R1/R2$ ($\hat{W}_{s12}$)and $R0/R1$ ($\hat{W}_{s01}$), long PRT $R1/R2$ ($\hat{W}_{L12}$), and the hybrid estimators $\hat{W}_H$ and $\hat{W}_{\hat{H}}$. Biases as a function of input spectrum width are shown in the top panel, the error standard deviations in the middle, and the weights used for the hybrid estimators in the bottom. Note that the "input" W for the $\hat{W}_{\hat{H}}$estimator is $\hat{W}_S$, whereas for $\hat{W}_H$ the simulator input W is used.
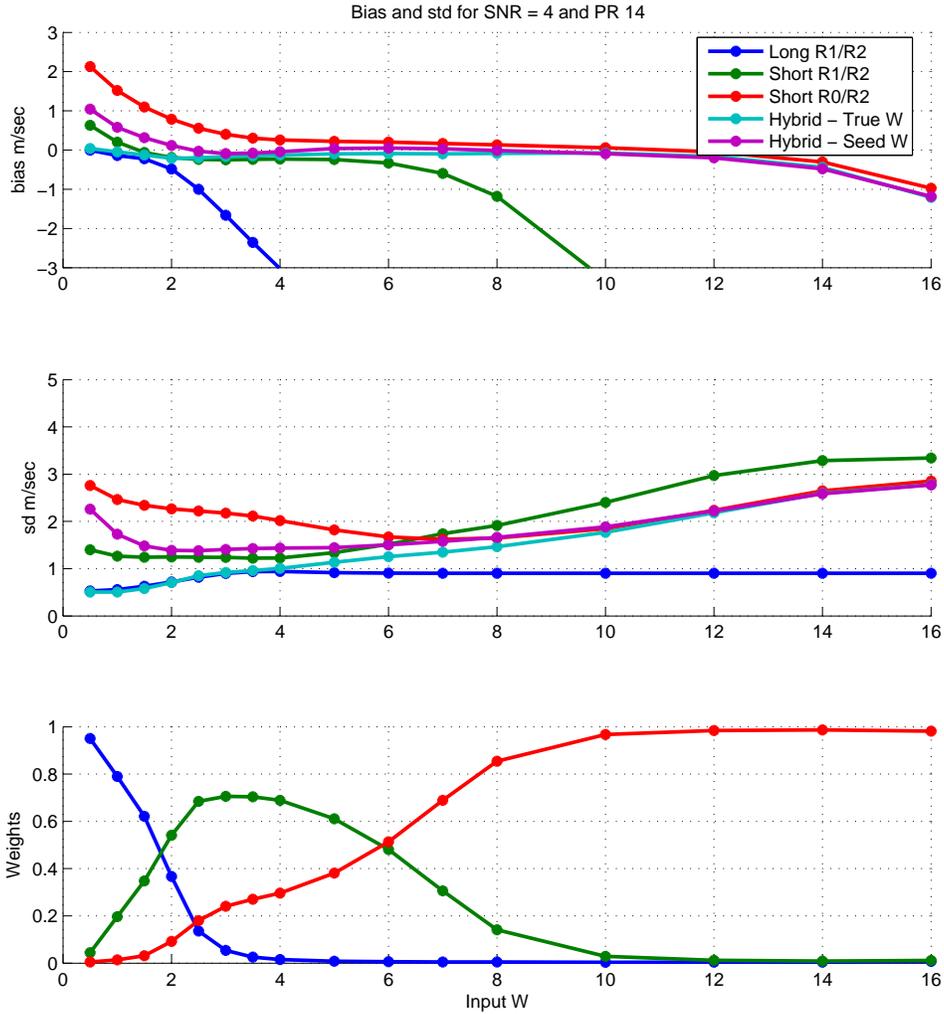
Figure 9: Performance statistics plots for 4 dB SNR and 14 dB PR, for the short PRT $R1/R2$ ($\hat{W}_{s12}$) and $R0/R1$ ($\hat{W}_{s01}$), long PRT $R1/R2$ ($\hat{W}_{L12}$), and the hybrid estimators $\hat{W}_H$ and $\hat{W}_{\hat{H}}$. Biases as a function of input spectrum width are shown in the top panel, the error standard deviations in the middle, and the weights used for the hybrid estimators in the bottom. Note that the "input" W for the $\hat{W}_{\hat{H}}$ estimator is $\hat{W}_S$, whereas for $\hat{W}_H$ the simulator input W is used.
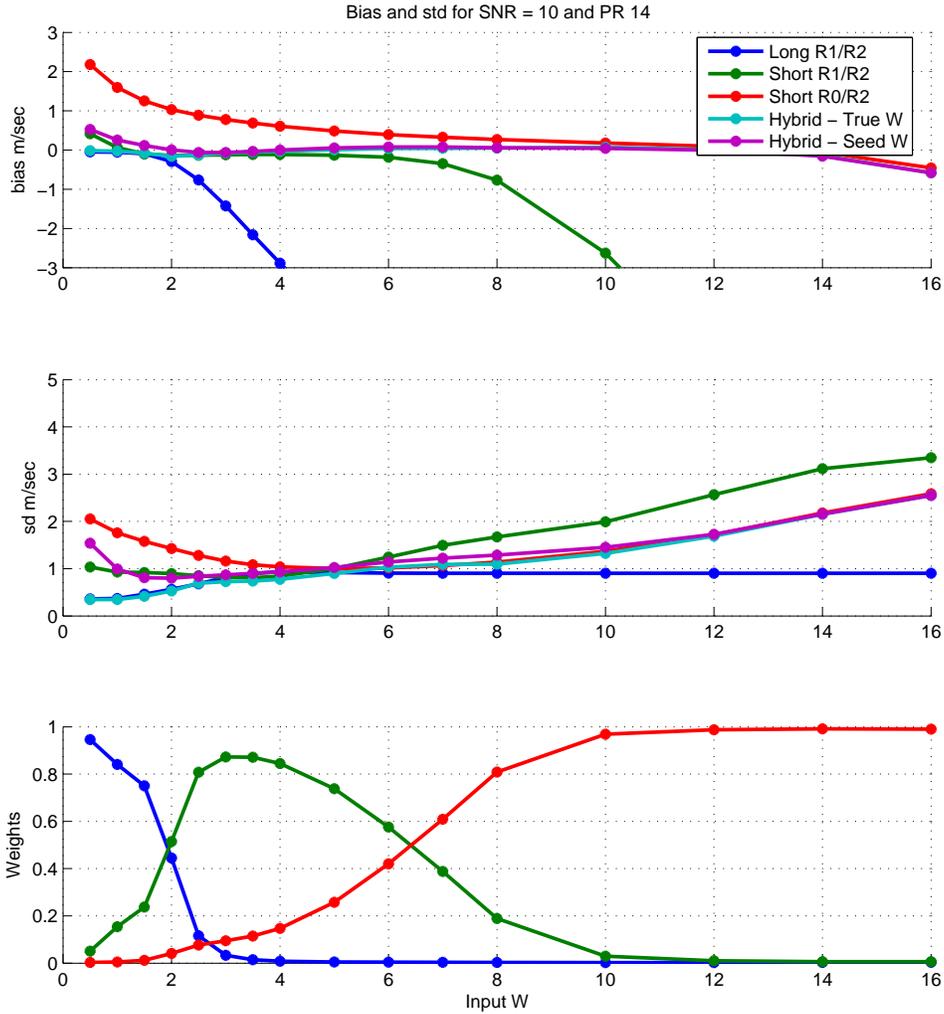
Figure 10: Performance statistics plots for 10 dB SNR and 14 dB PR, for the short PRT $R1/R2$ ($\hat{W}_{s12}$) and $R0/R1$ ($\hat{W}_{s01}$), long PRT $R1/R2$ ($\hat{W}_{L12}$), and the hybrid estimators $\hat{W}_H$ and $\hat{W}_{\hat{H}}$. Biases as a function of input spectrum width are shown in the top panel, the error standard deviations in the middle, and the weights used for the hybrid estimators in the bottom. Note that the "input" W for the $\hat{W}_{\hat{H}}$ estimator is $\hat{W}_S$, whereas for $\hat{W}_H$ the simulator input W is used.